Microwave and
Optical Technology Letters

A Low-Profile 28-GHz Rotman Lens-Fed Array Beamformer for 5G Conformal Subsystems

Journal:	*Microwave and Optical Technology Letters*
Manuscript ID	MOP-18-0897
Wiley - Manuscript type:	Research Article
Date Submitted by the Author:	27-Jul-2018
Complete List of Authors:	Rahimian, Ardavan; Queen Mary University of London, School of Electronic Engineering and Computer Science Abbasi, Qammer; University of Glasgow, School of Engineering Alomainy, Akram; Queen Mary University of London, School of Electronic Engineering and Computer Science Alfadhl, Yasir; Queen Mary University of London, School of Electronic Engineering and Computer Science
Keywords:	5G, beamforming network, conformal antenna array, Rotman lens, wireless subsystem

A Low-Profile 28-GHz Rotman Lens-Fed Array Beamformer for 5G Conformal Subsystems

Ardavan Rahimian, Qammer H. Abbasi, Akram Alomainy, and Yasir Alfadhl

***Abstract*—This paper reports on the first demonstration of an experimental millimeter-wave (mm-wave) beamforming based on the conformal Rotman lens (RL)-fed array feeding concept. The passive switched-beam network is intended for operation in the 28-GHz band, covering the 18–38 GHz range, for the deployment in the fifth generation (5G) subsystems. The primary objective of this work is to conduct the feasibility of designing a beamforming network (BFN) based on liquid-crystal polymer (LCP) substrate, and to evaluate the performances in terms of the scattering (*S*)-parameters and surface currents for the proposed flexural case of the convex-circumferential bending (i.e., the conformal flexure). A prototype has been accurately fabricated, and a setup has also been deployed to conduct the measurements. The performance in terms of the linear progressive phase behavior, as the main figure of merit, has been shown. The developed BFN exhibit significant characteristics to be used as a low-profile unit of the transceivers with the in-built beam steering for the conformal 5G subsystems.**

***Index Terms*—5G, beamforming network, conformal antenna array, mm-wave, low-profile, Rotman lens, wireless subsystem.**

I. Introduction

THE advanced smart antenna technologies developed based on the emerging radio frequency (RF) subsystems provide the 5G ultra-dense networks (UDN) infrastructures with the essential requirements for the purpose of optimal RF operation and propagation based on the front-end arrays. Employment of the electromagnetic (EM) systems consequently results in the improvement of the network performance that is evaluated in terms of the improved signal-to-noise ratio (SNR), which also increases the achievable information capacity and throughput, and thus expediting the required Gbps data transmission rate among the access point (AP) links [1, 2]. This can be achieved through combining the directional, narrow, and high-gain RF beams, to effectively increase the array gain in the direction of interest (i.e., to enhance the coverage, and to maximize the RF signal strength), as well as to realize the spatial diversity as the signal moves throughout the sector; the latter is also based on minimizing the multipath fading by using the beam steering functionality toward a desired signal and further steering a null toward an interfering one. In this regard, generating multiple beams using an array along with having wide bandwidth and electronic beam steering capability are of crucial importance for the 5G communication systems [2, 3]. For this purpose, the lens-based switched-beam networks are effectively employed to have control over the amplitude and phase at each element of the antenna array [4, 5]. This would lead to the feasibility of implementing the networks according to the aerodynamic and hydrodynamic properties of the site-specific bearing surfaces, as well as the configurations of the intended infrastructures at the APs [6, 7]. This work has undertaken the thorough design and performance analysis of a lens-fed BFN that is bent under the introduced conformal flexure, to be used in the integrated modules for the 5G systems [2, 8]. This concept has emerged from the conformal antennas fed by the planar lenses [9].

Manuscript received July 27, 2018;

A. Rahimian, A. Alomainy, and Y. Alfadhl are with the School of Electronic Engineering and Computer Science, Queen Mary University of London, London E1 4NS, U.K. (e-mail: a.rahimian@qmul.ac.uk).

Q. H. Abbasi is with the School of Engineering, University of Glasgow, Glasgow G12 8QQ, U.K.

II. 5G RL-BFN: Theoretical Design and Analysis

The RL has been designed based on the 5 × 8 configuration, in which the LCP-based 28-GHz RL beamformer incorporates five input (i.e., beam) ports and eight output (i.e., array) ports, suitable for an eight-element antenna array, along with eight dummy ports, in order to absorb the energy, and to reduce the reflections on each side of the lens cavity. The lens device has the scan angle of ±30° with the half-wavelength array element spacing. For the sake of brevity, the details of the BFN design frameworks are not provided, as they are thoroughly discussed in [7, 8]. The operation of the lens has been analyzed through the high-performance computing (HPC)-centric full-wave EM simulations, conducted based on the robust time-domain finite integration technique (FIT) using the EM transient solver (i.e., the CST STUDIO SUITE software). This has been performed to evaluate the time-domain characteristics of this electrically-large structure. Fig. 1 shows the simulated EM characteristics of the BFN based on the introduced conformal flexural case of the convex-circumferential bending, in which the beamformer is bent around a cylinder of radius R = 60 mm, while exerting the minimum and maximum device efficiencies of 56.7% and 58.2% at the frequency of 28-GHz (i.e., numerically computed based on the equations given in [7]) when beam ports one and three are excited, respectively. Fig. 2 also illustrates the phase behavior of the RL under the same conditions of the beam port excitations and flexure. It shows the linear behavior across the output array contour, confirming the usability for the RF beam steering. The transmission lines (TLs) connected to the array ports have also been extended and meandered, to maintain an identical electrical length among the output array elements.

III. 5G RL-BFN: Experimental Design and Analysis

In order to experimentally validate the designed RL-BFN, a lens prototype has been accurately fabricated using the LPKF ProtoLaser U4 to deploy the laser-based micromaterial and RF circuit structuring technique, and to further maintain the high-resolution realization required for the optimal RF performance of the lens. This technique has been conducted to minimize the non-uniformity of the TLs, as well as the fabrication errors, in comparison with the other implementation methods. The lens device has been realized on the Rogers ULTRALAM 3850HT flexible LCP substrate, with the dielectric constant of $\varepsilon_r = 2.9$, loss tangent of $\tan\delta = 0.0025$, substrate thickness of $h = 0.18$ mm, and copper cladding of $t = 17.5$ μm, as in [5, 7]. Figs. 4 and 5 show the simulated and realized RL-BFN, as well as the measurement setup for the subsystem testing respectively. The measurements have been carried out using the in-house vector network analyzer (VNA), i.e., Keysight Technologies PNA-X, to measure both the magnitude and phase properties of the RL device. It should be noted that the Pasternack PE44489 mini-SMP male connectors have been used for the measurements, as well as the thin and flexible microwave absorbing material (i.e., ECCOSORB FGM-40) for terminating the ports, except the ones under the test. This mechanism has been proposed for the device to introduce an additional degree of freedom for the integration of the circuits and systems at the transceiver level, to reduce the complexity and overhead of the measurements, and to reduce the cost of the subsystem implementation at the mm-wave frequency bands. As Fig. 3 presents, the absorber is used as an efficient method for terminating the ports instead of using a large number of connectors and 50-Ω loads. Moreover, in order to assess the performance of the wideband absorber at the intended frequency band (i.e., 17–20 GHz), the absorbing material has been accurately characterized using the deployed setup based on the dielectric probe technique, and the obtained data have been further loaded into a developed LCP-based TL model, as also realized in the lens, to examine the performance of the absorbing material in terms of the effective attenuation and reflectivity in a wideband RF frequency domain.

Moreover, for the purpose of experimentally validating the full-wave simulations for the conformal flexure of the convex circumferential bending, the realized 28-GHz beamformer has been employed to appropriately conduct the beamforming, and to be rigorously measured for the evaluation of the RF output performance of the RL in the conformal case. In this regard, a setup has been accurately deployed for the RL to be placed for the measurements using the VNA. The lens has been then bent around a cylinder of radius $R = 60$ mm, and the measurements have been carried out (i.e., Fig. 6) to obtain the magnitude and phase characteristics of the RL. Also, the generation of the RF beams in different orientations results in the provision of the versatility and robustness in mm-wave communications, along with the optimized and symmetrical EM radiation patterns, in response to the RF propagation environment in the imperfect channels encountering the multipath, interference, and fading.

Fig. 7 shows the measured phase behavior of the planar RL, in order to thoroughly confirm the functionality of the device to conduct the linear phase division required for the electronic beam steering. The measured results are in a good agreement with the simulated results throughout the operating band. The slight deviations are mainly due to the errors and mismatches caused by the cables, SMPM adapters, and soldering. Fig. 8 shows the measured output characteristics under the conformal condition. The RL device exhibits a significant performance in terms of the wideband operation and linear phase distributions across the array contour. This can be exploited further for the integration at the transceiver level to fully realize an integrated phased array module for the potential use in the 5G systems.

IV. Conclusion

This letter has demonstrated the first experimental wideband mm-wave beamforming based on a low-profile conformal 28-GHz Rotman lens-fed array BFN. This RL exhibits significant performances in terms of the essential functional requirements for the electronic beam steering in the 5G conformal systems.

References

[1] M. Xiao *et al.*, "Millimeter wave communications for future mobile networks," *IEEE J. Selected Areas Commun.*, vol. 35, no. 9, pp. 1909–1935, Sep. 2017.

[2] W. Hong *et al.*, "Multibeam antenna technologies for 5G wireless communications," *IEEE Trans. Antennas Propag.*, vol. 65, no. 12, pp. 6231–6249, Dec. 2017.

[3] Y. Gao *et al.*, "Rotman lens based hybrid analog-digital beamforming in massive MIMO systems: Array architectures, beam selection algorithms, and experiments," *IEEE Trans. Vehicular Tech.*, vol. 66, no. 10, pp. 9134–9148, Oct. 2017.

[4] O. Kilic and S. J. Weiss, "Rotman lens applications for the US Army: A review of history, present, and future," *URSI Radio Sci. Bull.*, vol. 2010, no. 332, pp. 10– 23, Jun. 2010.

[5] J. Saily *et al.*, "Millimetre-wave beam-switching Rotman lens antenna designs on multi-layered LCP substrates," in *10th European Conf. Antennas Propag.*, Apr. 2016, pp. 1–5.

[6] T. K. Vo Dai and O. Kilic, "Compact Rotman lens structure configurations to support millimeter wave devices," *Progress In Electromagn. Res. B*, vol. 71, pp. 91–106, 2016.

[7] A. Rahimian, Y. Alfadhl, and A. Alomainy, "Analytical and numerical evaluations of flexible V-band Rotman lens beamforming network performance for conformal wireless subsystems," *Progress In Electromagn. Res. B*, vol. 71, pp. 77–89, 2016.

[8] A. Rahimian, Y. Alfadhl, and A. Alomainy, "Design and performance analysis of millimetre-wave Rotman lens-based array beamforming networks for large-scale antenna subsystems," *Progress In Electromagn. Res. C*, vol. 78, pp. 159–171, 2017.

[9] A. Mahmoodi and A. Pirhadi, "Enhancement of scan angle using a Rotman lens feeding network for a conformal array antenna configuration," *ACES J.*, vol. 30, no. 9, pp. 959–966, Sep. 2015.

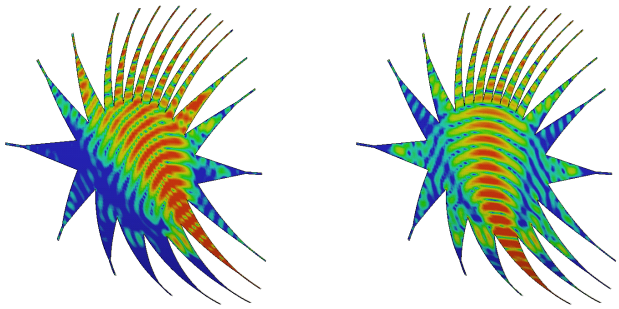

(a) (b)

Fig. 1. Surface current distributions of the conformal lens for the excited input beam ports at center frequency f = 28-GHz: (a) port one; (b) central port three. The scale for the magnetic strength is 10–30 ampere per meter (1 A/m) in dB.

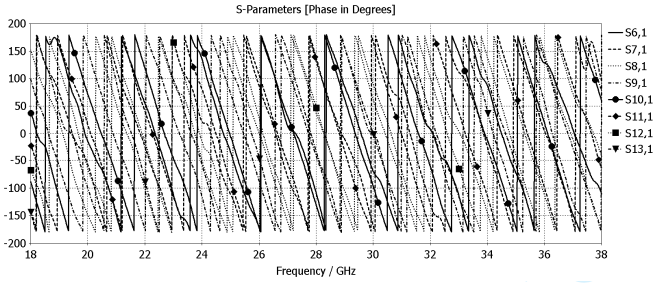

(a)

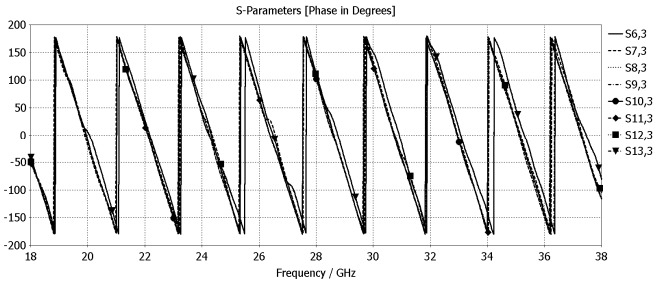

(b)

Fig. 2. Characteristics of the 28-GHz RL based on the conformal flexural case of the convex-circumferential bending: (a) linear phase distributions for the excited beam port one; (b) linear phase distributions for the excited port three.

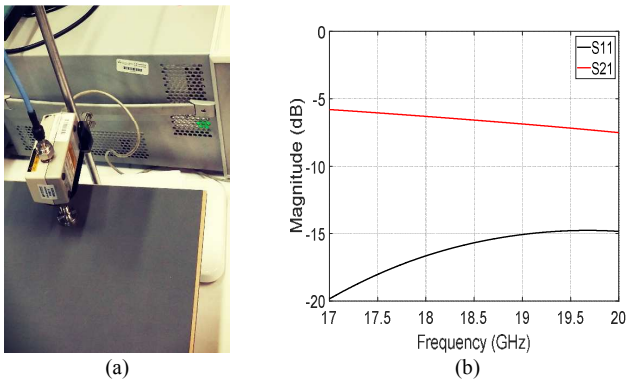

(a) (b)

Fig. 3. RF absorber characterization: (a) setup based on the probe technique for measuring the properties; (b) output performance based on the loaded data.

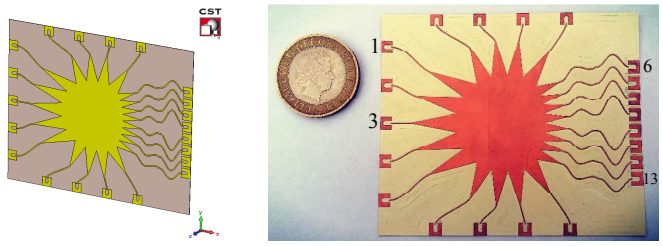

(a) (b)

Fig. 4. LCP-based 28-GHz 5 × 8 RL, with dimensions of 75.45 × 89.87 mm^2: (a) simulated prototype, perspective view; (b) fabricated prototype, front view.

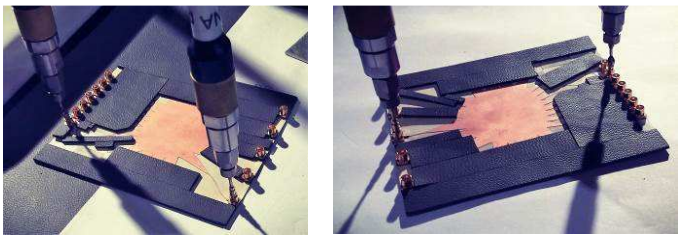

(a) (b)

Fig. 5. Experimental wideband beamforming for 5G applications, based on the planar LCP-based 28-GHz 5 × 8 RL: (a) subsystem under test (SUT) for input beam port one active; (b) SUT for the excited central input beam port three.

(a) (b)

Fig. 6. Experimental wideband beamforming for 5G applications, based on the conformal LCP-based 28-GHz 5 × 8 RL: (a) SUT setup for central input beam port three active, top view; (b) deployed SUT, perspective view.

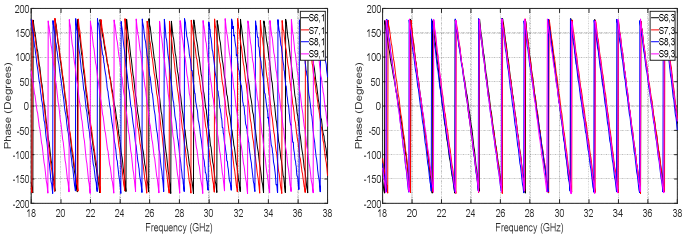

(a) (b)

Fig. 7. Measured *S*-parameters of the wideband planar 28-GHz RL-BFN, in terms of the linear progressive phase distributions required for beam steering: (a) input beam port one active; (b) central input beam port three active.

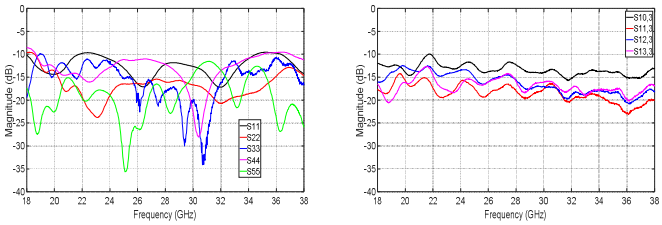

(a) (b)

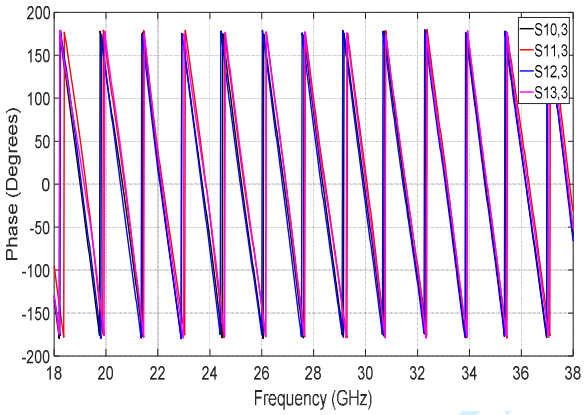

(c)

Fig. 8. Measured *S*-parameters of the wideband conformal 28-GHz RL: (a) reflection coefficients for the excited input ports; (b) transmission coefficients for port three active; (c) linear phase distributions for central port three active.